Mode coupling and fragile to strong transition in supercooled TIP4P water

P. Gallo and M. Rovere

Citation: J. Chem. Phys. **137**, 164503 (2012); doi: 10.1063/1.4759262
View online: http://dx.doi.org/10.1063/1.4759262
View Table of Contents: http://jcp.aip.org/resource/1/JCPSA6/v137/i16
Published by the American Institute of Physics.

Mode coupling and fragile to strong transition in supercooled TIP4P water

P. Gallo and M. Rovere
Dipartimento di Fisica, Università "Roma Tre" Via della Vasca Navale 84, 00146 Roma, Italy

(Received 27 July 2012; accepted 2 October 2012; published online 23 October 2012)

We consider one of the most used model for water, the rigid four site TIP4P potential, and we study by molecular dynamics simulation the dynamical properties of the liquid upon supercooling. In the previous studies of the thermodynamics of the TIP4P model a liquid-liquid critical point (LLCP) located at the end of the coexistence between the low density liquid (LDL) and the high density liquid (HDL) of water was found. We present here the analysis of the self intermediate scattering functions in a large range of temperatures and densities and we show that the structural relaxation in the region of mild supercooling is in agreement with the predictions of the mode coupling theory. In the more deep supercooled region we observe that the α-relaxation time deviates from the mode coupling theory (MCT) trend and a crossover takes place from a fragile to a strong behavior upon crossing the Widom line emanating from the LLCP. The HDL and the LDL phases are associated with the fragile and the strong behavior, respectively. © *2012 American Institute of Physics*. [http://dx.doi.org/10.1063/1.4759262]

I. INTRODUCTION

The behavior of supercooled liquid water is a matter of vivid debate. An huge amount of experimental, theoretical, and computational work has been performed in order to explain the anomalies of this liquid that plays an important role in many fields of physics, chemistry, and biology. Besides the well known presence of a temperature of maximum density (TMD) a peculiar increase of different thermodynamic response functions in metastable liquid water has been revealed in experiments. Extrapolations of the data toward a singular temperature $T_S = -45^\circ$ C show apparent power law divergences of the specific heat and the isothermal compressibility, typical of a phase transition.[1] Experiments in the region of deep supercooling are extremely difficult due to nucleation processes. For this reason it was impossible to discriminate between the different hypothesis formulated to explain the water anomalies. On the basis of a number of computer simulation studies started with the pioneering work on ST2 water,[2,3] the hypothesis of a second critical point of water has received much attention in alternative to other interpretation like the singularity free scenario.[4] Simulations with different models for water have shown the possibility of the existence of a liquid-liquid coexistence terminating in a liquid-liquid critical point (LLCP), see for instance Refs. 5–11. The LLCP scenario however is still in the heart of a lively debate.[1,8,12–17]

The idea behind the liquid-liquid coexistence is related to the experimental observation of water polyamorphism.[18–20] Two coexisting phases of glassy water, the low density amorphous (LDA), and the high density amorphous ice, would transform at increasing temperature in two coexisting metastable liquid phases, the low density liquid (LDL) and the high density liquid (HDL). The coexistence line between LDL and HDL would terminate into a LLCP, approximately located at $T \approx 220$ K and a pressure $P \approx 100$ MPa, as estimated from extrapolation of experimental results.[21,22]

In 1996 it was also shown that SPC/E water was behaving like a simple liquid glass former[23,24] testing the mode coupling theory (MCT) of glassy dynamics.[25] Besides the MCT crossover temperature was close/coincident with the singular temperature T_S where dynamical and thermodynamic properties showed a divergence, already pointing to a strong connection between dynamics and thermodynamics. MCT has been later shown to hold also for liquids in confinement[26,27] and in particular in confined water.[28–32]

Recently new interest in the comprehension of the behavior of supercooled water has been stimulated by a number of experiments on confined water, where crystallization can be more easily avoided upon supercooling. In experiments on water in MCM41 and water at interface with proteins[33–35] it has been found that the structural relaxation of the liquid approaching the glass transition changes from a fragile to a strong behavior, following the classification scheme of Angell.[36] This fragile to strong crossover (FSC) would be connected to the presence of the liquid-liquid coexistence and the presence of a LLCP. The FSC would be for water approaching the glass transition the signature of the passage from the fragile character of the HDL phase to the strong Arrhenius dynamics of the LDL phase. A lively debate has grown on the interpretation of these experiments.[37–41] A number of computer simulations on bulk and confined water and in hydrophobic aqueous solutions in fact agree with the presence of a FSC in combination with the liquid-liquid transition.[7,14,31,32,42,43]

According to the interpretation of Ref. 7, the approach to the LLCP from the single phase region would be indicated by an anomalous increase in quantities like the isothermal compressibility and the specific heat. The maxima of these functions would collapse on a single curve, called the Widom line (WL), that finally would terminate at the critical point. This is in analogy with the liquid-gas transition where the WL can be found for simple system by analytical and computer

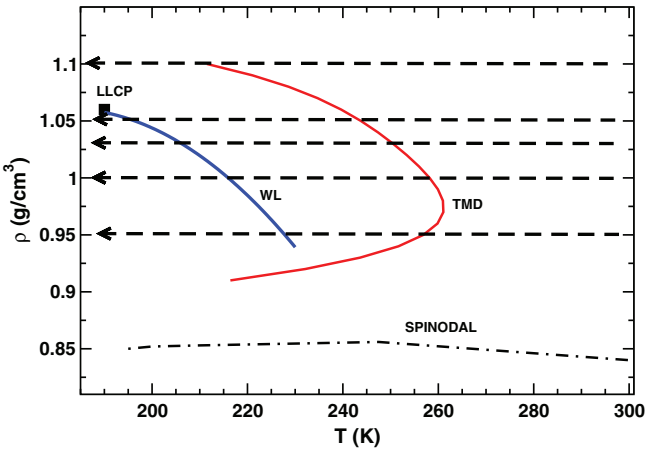

FIG. 1. Phase diagram of TIP4P water in the (T, ρ) plane, as adapted from Ref. 9. The nose shaped curve represents the temperature of maximum density (TMD). The dot dashed line is the low temperature liquid-gas spinodal The continuous line is the Widom line (WL) defined in the text. The point indicated as LLCP is the estimated location of the liquid-liquid critical point. The dashed line with arrows mark the paths and the direction along which the MD simulation has been performed.

simulation methods.[44–46] In supercooled water close to the LLCP the presence of a WL would affect the dynamical behavior of water. The FSC, in fact, would take place when the supercooled water crosses the WL.[7]

Between the class of rigid models that can be used for water TIP4P[47] has been extensively used for studying supercooled pure water and aqueous salt solutions.[9,48–51] It works well in reproducing the thermodynamic and structural properties of water[52,53] and recently it has been shown that the phase diagram of water in an extended range of pressures and temperatures can be obtained by a rigid shift of the TIP4P phase diagram to make the TIP4P TMD line coincide with the experimental TMD.[9,54]

In the calculations of the phase diagram in the region of the supercooled liquid it was found that TIP4P water shows a liquid-liquid coexistence and the LLCP was estimated from the behavior of the isochores and the isotherms.[9] The phase diagram is shown in Fig. 1 in the $T - \rho$ plane. We found the LLCP to be located at $T = 190$ K, $P = 150$ MPa, and $\rho = 1.06$ g/cm^3. In the same figure the WL is reported. In this paper we focus on the dynamical properties of TIP4P water upon supercooling with the aim to connect the relaxation dynamics to the thermodynamic peculiarities found in our previous work. For this reason we performed molecular dynamics (MD) simulation along thermodynamic paths approaching the Widom line.

In Sec. II, we present the model and the details of the simulations. In the Sec. III, we describe the behavior of the relaxation time and of the diffusion. In Sec. IV, we describe the MCT behavior down to the crossover in dynamics. Section V is devoted to the analysis of the location of the FSC with respect to the Widom line. Section VI deals with the conclusions.

II. MODEL AND SIMULATION METHODS

We performed MD simulations with the TIP4P model for water, a rigid four site model, where hydrogens (H) are represented by two positively charged sites connected to a neutral oxygen (O) site. The negative charge of O is shifted by 0.15 Å in the molecular plane. The angle between the two O–H bonds is 104.51°. The interactions between the sites of the water molecules are determined by a combination of a Coulombic and a Lennard-Jones potential. Details about the parameters can be found in literature, see for instance Ref. 48. The interactions were truncated at 9 Å and the Ewald method was used to account for the long range electrostatic interactions.

We calculated the self intermediate scattering functions (SISF) and the mean square displacement (MSD) at the densities $\rho = 0.95$, 1.00, 1.03, 1.05, 1.10 g/cm^3 along the paths represented in Fig. 1 from $T = 300$ K down to $T = 190$ K. Apart for $\rho = 1.10$ g/cm^3 the paths cross the WL obtained in the previous work from the maxima of the constant volume specific heat c_v.[9] In the calculation for bulk TIP4P water the WL obtained from the maxima of c_v and from the maxima of the isothermal compressibility are very close to each other, the WL from c_v, however, was less affected by fluctuations with respect to the line calculated from the isothermal compressibility. Besides in previous calculations on confined water we found that the FSC was located close to the maxima of the constant volume specific heat.[31]

The dynamical quantities were obtained from MD simulations performed in the microcanonical ensemble with a timestep of 1 fs after equilibration with the use of the Berendsen thermostat.

III. RELAXATION TIME AND DIFFUSION

The SISF, calculated at the peak position of the static structure factors $Q_0 = 2.25$ Å^{-1} for the oxygens, are reported in Fig. 2 for the density $\rho = 1.00$ g/cm^3. The double relaxation regime typical of supercooled liquids is observed at decreasing temperatures. After the initial ballistic decay the system enters in the β-relaxation region at intermediate times and then in the α-relaxation region at long times. This behavior

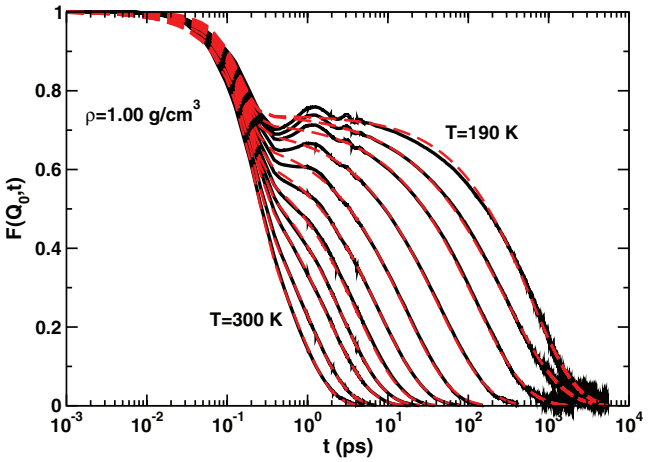

FIG. 2. Oxygens self intermediate scattering function (SISF) calculated at the position Q_0 of the maximum of the static structure factor for the density $\rho = 1.00$ g/cm^3 and temperatures from $T = 300$ K to $T = 190$ K. The black bold curves are the MD results, while the dashed curves are the fits with Eq. (1).

TABLE I. Fitting parameters of the SISF with Eq. (1) and values of the diffusion coefficient D for the density $\rho = 1.00$ g/cm^3.

T (K)	A	r_{cage} (Å)	τ_s (ps)	τ (ps)	β	D (10^{-5} cm^2/s)
300	0.661	0.495	0.213	0.644	0.923	3.77
280	0.660	0.496	0.211	0.936	0.857	2.13
260	0.653	0.502	0.202	1.662	0.801	1.22
250	0.643	0.511	0.192	2.586	0.809	0.797
240	0.644	0.511	0.185	4.318	0.800	0.539
230	0.663	0.493	0.177	7.648	0.762	0.337
220	0.683	0.475	0.167	15.93	0.745	0.169
210	0.709	0.451	0.157	41.38	0.700	$7.1\ 10^{-2}$
200	0.723	0.438	0.152	121.7	0.689	$2.6\ 10^{-2}$
195	0.745	0.418	0.146	287.5	0.626	$1.2\ 10^{-2}$
190	0.738	0.424	0.149	606.4	0.770	$6.4\ 10^{-3}$

can be understood in terms of the "cage effect." As temperature is lowered particles start being trapped in the transient cage formed by their nearest neighbors. After the ballistic time region the particles remain trapped in the cage and when the cage relaxes they are free to diffuse again.

The curves are fitted with the equation[23,24]

$$f(Q,t) = (1-A(Q))\exp[-(t/\tau_s)^2] + A(Q)\exp[-(t/\tau)^\beta], \tag{1}$$

this formula combines the short time fast relaxation determined by the relaxation time τ_s, the long time α-relaxation described by the stretched exponential containing the long time relaxation τ and the Kohlrausch exponent β. The normalizing coefficient $A(Q)$ corresponds to the Lamb-Mössbauer factor[25,55] and its value is related to the "cage effect" since $A(Q) = \exp(-r_{cage}^2 Q^2/3)$ where r_{cage} is the cage radius.

The fitting parameters for this density are reported in Table I. The parameters are in the range of that observed for SPC/E water[23,24,56] and show a similar trend except for the cage radii and the fast relaxation times. We observe a shrinkage of the cage upon decreasing temperature below 240 K and correspondingly a decrease of the fast relaxation time in our case, while they are approximately constant for SPC/E.[23,24] In the MCT framework β should decrease from 1 at high temperatures and approach the value of the von Schweidler exponent b, upon approaching the MCT crossover temperature. But close to this temperature hopping intervenes introducing deviations from MCT (see Sec. IV).

In Fig. 3, we report the MSD $\langle \Delta r^2(t) \rangle = \langle |r(t) - r(0)|^2 \rangle$ for the density $\rho = 1.00$ g/cm^3 on a log-log plot. It is evident that as the temperature goes down a plateau appears after an initial ballistic regime and before the onset of the Brownian regime where the MSD becomes proportional to the time according to the Einstein relation $\langle \Delta r^2(t) \rangle = 6Dt$. From the behavior at long time the diffusion coefficients D are extracted and reported in Table I. We also observe that the onset of the cage appears at around $t = 0.25$ ps regardless of the temperature and analogous to SPC/E water.

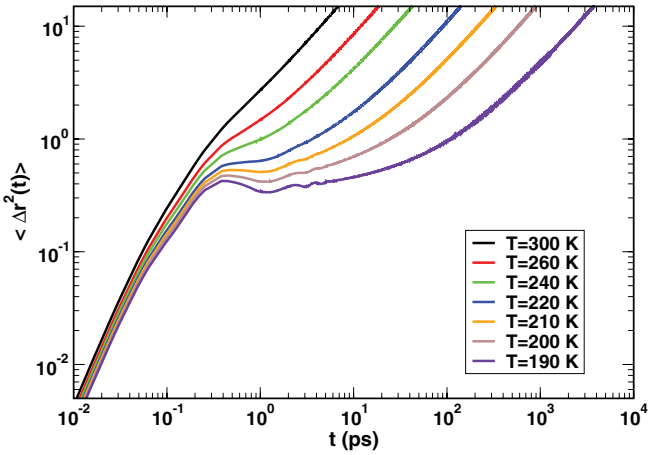

FIG. 3. Mean square displacement for density $\rho = 1.00$ g/cm^3 and temperatures from $T = 300$ K to $T = 190$ K.

IV. MCT TRANSITION AND FRAGILE TO STRONG CROSSOVER

According to MCT the two step relaxation found in the SISF can be interpreted in terms of an approach of the system to an ideal transition from an ergodic to a non-ergodic behavior as the temperature goes down to the crossover value T_C. This temperature marks the change from a regime where relaxation processes in the liquid are mastered by breaking and reforming of the cages to a regime where the cages are frozen and diffusion is attained through hopping. From the fitting procedure described above we can derive the behavior of the α-relaxation time as function of temperature. It is found that τ follows the MCT prediction and it can be fitted with a power law behavior

$$\tau \sim (T - T_C)^{-\gamma}. \tag{2}$$

The divergence takes place in the asymptotic limit. This limit is never reached and the divergence is smeared out due to the hopping effects neglected in the ideal version of MCT. As a consequence of Eq. (2) since the diffusion coefficient $D \sim \tau^{-1}$, it is predicted that D goes to zero with the power law $D \sim (T - T_C)^\gamma$.

As reported in Fig. 4, for the density $\rho = 1.00$ g/cm^3, τ can be fitted with Eq. (2) with $T_C = 191$ K and $\gamma = 2.54$ well within the range predicted by MCT $\gamma > 1.7666$. The fit can be performed by excluding the lowest temperatures. This is evidenced in the inset of Fig. 4, where the MCT fit is reported in a log-log plot. For this density around $T = 214$ K it is observed a crossover from a MCT (fragile) to an Arrhenius (strong) behavior described by the equation

$$\tau = \tau_0 e^{E_A/k_B T}, \tag{3}$$

where E_A is the activation energy.

We will discuss this point below in connection with the results for the other densities.

A further test of the MCT prediction is provided by the time-temperature superposition principle (TTSP). In the time region corresponding to the late β-relaxation and early α-relaxation according to MCT the SISF must satisfy the scaling

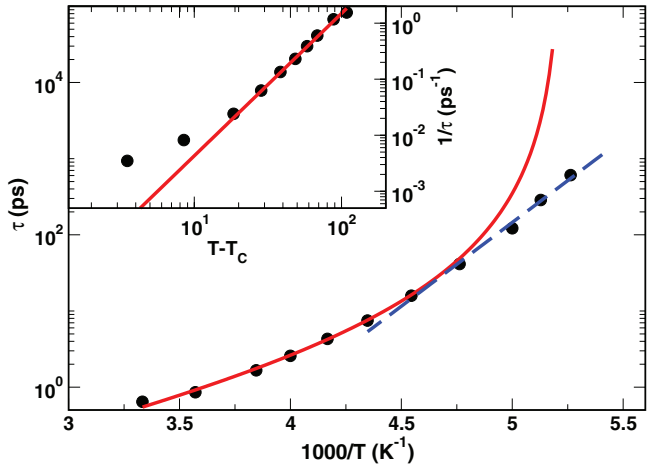

FIG. 4. α-relaxation time τ as function of the inverse temperature for $\rho = 1.00$ g/cm^3. The continuous curve is the fit with the MCT prediction, Eq. (2). The dashed line is the fit with the Arrhenius function (3). In the inset Log-log plot of the inverse of τ vs $T - T_C$.

relation, called von Schweidler law (VSL),

$$F(Q,t) = \hat{\phi}_Q\,(t/\tau)\,, \tag{4}$$

where $\hat{\phi}_Q$ is a master function. The master function depends on the scaled time $\tilde{t} = t/\tau$ and has the form

$$\hat{\phi}_Q(\tilde{t}) = f_Q^c - h_Q \cdot (\tilde{t})^b, \tag{5}$$

where b is the von Schweidler exponent, f_Q^c is the non-ergodic parameter and h_Q is the amplitude factor. We rescaled the time dependence of the SISF at $Q = Q_0$ with the τ previously extracted and in Fig. 5 it is evident that the SISF satisfy the TTSP in the range where the MCT is valid. The parameters obtained with the data collapsing on the single von Schweidler curve (5) are $f_Q^c = 0.671$, $h_Q = 0.427$, and $b = 0.55$. The von Schweidler exponent b is related in the framework of the MCT to the other parameters of the theory, the exponent parameter λ and the critical exponent a from the exact

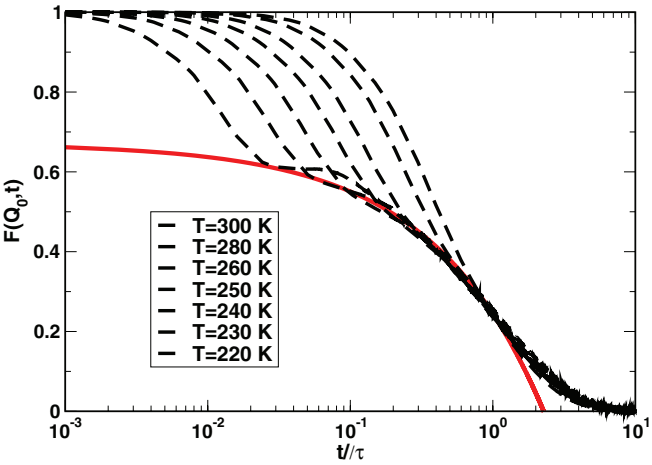

FIG. 5. SISF for the density $\rho = 1.00$ g/cm^3, at $Q = Q_0$ in the range of temperatures where MCT holds and scaled by the τ obtained from the fit (1). The continuous line is the fit to the VSL, Eq. (4). The parameters of the fit are reported in the text.

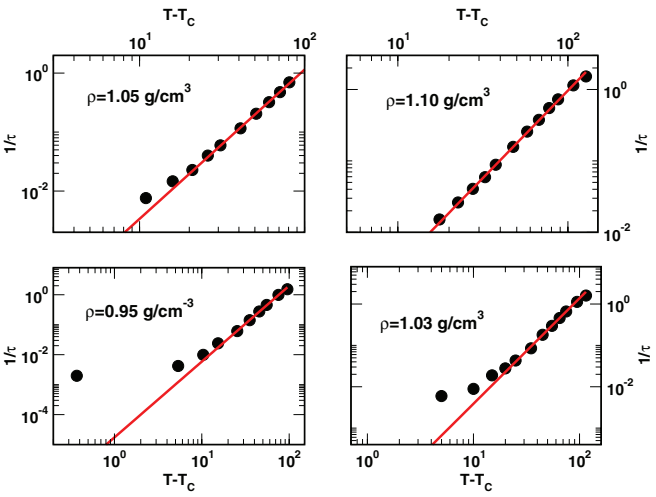

FIG. 6. Log-log plot of the inverse of the α-relaxation time $1/\tau$ versus $T - T_C$ (black points) for different densities, as indicated in the panels. The continuous line represents the MCT fit with Eq. (2). The plots report the values for which $T > T_C$. For each panel the scale is chosen in order to make more evident the fit to the MCT prediction. The complete behavior of τ as function of T is reported in Fig. 7.

relations

$$\lambda = \frac{\Gamma^2(1+b)}{\Gamma(1+2b)} = \frac{\Gamma^2(1-a)}{\Gamma(1-2a)}, \tag{6}$$

$$\gamma = \frac{1}{2a} + \frac{1}{2b}, \tag{7}$$

where in (6) $\Gamma(x)$ is the Euler Γ-function and in (7) γ is the exponent in Eq. (2). The parameters must be in the ranges $1/2 < \lambda < 1.0$, $0 < a < 0.395$ and $0 < b < 1$. Since only one parameter is independent, to test MCT we calculate from the value of b in (6) the other parameters and we get $\lambda = 0.75$ and $a = 0.30$ and from Eq. (7) we obtain $\gamma = 2.57$. This value is in agreement with the value $\gamma = 2.54$ directly obtained from the fit of the τ to the power law (2).

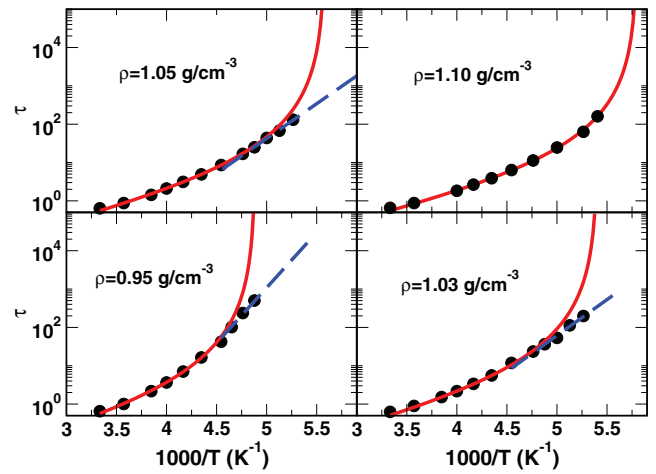

FIG. 7. α-relaxation time τ versus inverse temperature (black points) for different densities, as indicated in the panels. The continuous curve is the fitting with the MCT power law (2), the dashed curve is the fitting to the Arrhenius function (3).

TABLE II. Fit parameters of the MCT power laws for τ and D.

ρ (g/cm^3)	T_C (K) (τ)	T_C (K) (D)	γ (τ)	γ (D)
0.95	204.6	205.0	2.53	2.17
1.00	191.5	192.2	2.54	2.07
1.03	185.0	184.9	2.55	2.17
1.05	179.07	178.4	2.53	2.29
1.10	172.4	173.0	2.45	2.10

V. FRAGILE TO STRONG CROSSOVER AT THE WIDOM LINE

We discuss now the results for the other densities. We performed the same analysis just presented for $\rho = 1.00$ g/cm^3 along the paths reported in Fig. 1. For each density below $\rho = 1.10$ g/cm^3 the system approaches the WL. A further simulation has been performed at the density $\rho = 1.10$ g/cm^3 where the system is above the WL in the region of the HDL.

We applied the fitting procedure (1) to all the SISF and the results for the α-relaxation time are reported in Figs. 6 and 7.

In Fig. 6, it is evident that τ follows the MCT prediction for all the densities. The fitting parameters to the MCT law are reported in Table II, where we added also the values obtained by fitting the behavior of D. We notice that the T_C values derived from the fits to the power law of τ and D are very similar, while the exponents γ for D are systematically lower than the γ values for τ. These discrepancies can be attributed to hopping effects that induce a violation of the proportionality of $D \sim \tau^{-1}$. This was observed in MCT analysis of different glass forming liquids, see for example, Refs. 57 and 58.

We also note that at density $\rho = 1.03$ g/cm^3 SPC/E gives, from D, $T_C = 186.3$ K and $\gamma = 2.83$,[23] very similar to $T_C = 184.9$ K and $\gamma = 2.17$ that we obtained, from D, at the same density for TIP4P water.

As seen in Table II, T_C drops down at increasing density and we notice from Fig. 7 that the temperature at which τ deviates from the MCT prediction decreases at increasing density. Since deviations from the ideal behavior of MCT are expected when hopping effects become relevant it is clear that hopping onset is shifted to lower temperatures as the density increases.

The temperature at which the system deviates from the MCT fragile behavior and enters into the Arrhenius strong regime can be identified as the point of the FSC. As evidenced in Fig. 7 this temperature, indicated as T_L, decreases at increasing density. In the strong regime τ can be fitted with the function (3). The values of activation energies E_A and the temperatures of the FSC T_L are reported in Table III for all the densities investigated. Due to the slope of the curves the crossover temperatures cannot be evaluated with very high precision and their values are reported in the table and in Fig. 8 with their error bars. This result confirms that also TIP4P water holds the picture found in several simulations and experiments.[7,14,31,33–35,42,43]

TABLE III. Activation energy and FSC temperatures.

ρ (g/cm^3)	E_A (kJ/mol)	T_L (K)
0.95	55.2	224.4 ± 1.0
1.00	42.1	217.2 ± 1.0
1.03	36.0	210.0 ± 1.5
1.05	34.7	200.0 ± 1.5

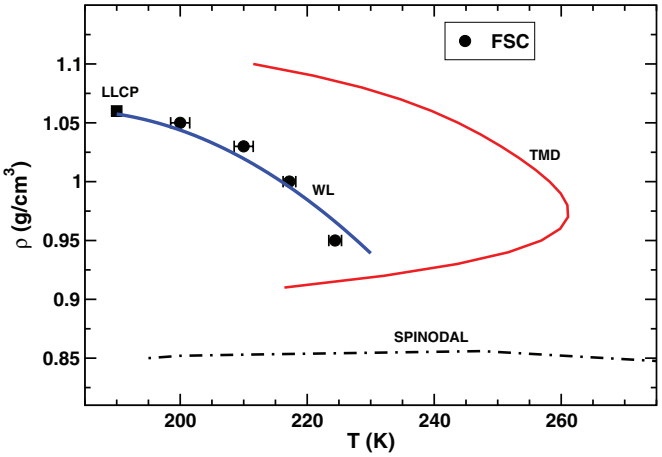

FIG. 8. Phase diagram of TIP4P water in the (T, ρ) plane, as adapted from Ref. 9. Symbols as 1. The points are the estimated location of the fragile to strong crossover.

The path along the density $\rho = 1.10$ g/cm^3 does not cross the WL, see Fig. 1, and τ keeps the fragile behavior down to the lowest temperature investigated, e.g., $T = 185$ K. Along the density paths crossing the WL the FSC appears to be equivalent to a cross over from the HDL to the LDL phases of water. This behavior is analogous to what found in studies of the Jagla particles.[7,43]

VI. CONCLUSIONS

We performed here MD simulations on a very popular and realistic model for water, the TIP4P, upon supercooling in a large range of temperatures and densities. We found that the system shows the properties of a supercooled liquid approaching the glass transition. The decay of the SISF $F_s(Q, t)$, calculated at each density at the Q corresponding to the maximum of the structure factor, can be described in terms of a double regime determined by a fast relaxation time τ_s and a slow relaxation time τ. The temperature has a strong effect on the τ, that increases by two order of magnitude going from $T = 300$ K down to 190 K. The slow relaxation of the SISF can be fitted with a stretched exponential form determined by the Kohlrausch exponent β. For a large portion of the temperature investigated the behavior of τ can be fitted with a power law in agreement with the prediction of the dynamics evolution of the MCT. τ diverges asymptotically at a temperature T_C that represents the ideal crossover from an ergodic to a nonergodic regime. Also the diffusion coefficient extracted from the study of the mean square displacement shows a behavior in agreement with MCT with values of T_C close to the values obtained for τ, while the Kohlrausch exponent β for D is

systematically lower with respect to corresponding β for τ. The behavior of τ deviates from the MCT prediction at a temperature T_L where it is observed a crossover toward an Arrhenius increase of τ typical of strong liquids. The ideal MCT is able to describe the dynamics in the fragile region, where hopping is not present. The asymptotic divergence of the α-relaxation time is smeared out by the appearance of hopping effects on approaching the region of deep supercooling where the liquid crosses to a strong behavior.

Importantly, we also found in our simulations that the FSC takes place along the WL in agreement with previous results obtained for different models of pure[7] and confined water[31] and of aqueous solutions.[43]

In the framework of the MCT theoretical approach the FSC can be interpreted in terms of a crossover from the ideal MCT behavior to the regime where hopping prevails. The calculations along the density paths approaching the LLCP from the single phase region indicate that the FSC is determined by the crossing of the Widom line. In the path passing only in the HDL phase the FSC is not observed down to the lowest temperature that was possible to equilibrate.

These results frame coherently in the picture indicating for water a strong connection between dynamics and thermodynamics and they confirm that also for TIP4P hopping is favored where water is less dense.[31,32]

ACKNOWLEDGMENTS

We gratefully acknowledge the computational support of CASPUR and the Roma Tre INFN-GRID.

[1] V. Holten, C. E. Bertrand, M. A. Anisimov, and J. V. Sengers, J. Chem. Phys. **136**, 094507 (2012).
[2] P. H. Poole, F. Sciortino, U. Essmann, and H. E. Stanley, Nature (London) **360**, 324 (1992).
[3] P. H. Poole, F. Sciortino, U. Essmann, and H. E. Stanley, Phys. Rev. E **48**, 3799 (1993).
[4] S. Sastry, P. G. Debenedetti, F. Sciortino, and H. E. Stanley, Phys. Rev. E **53**, 6144 (1996).
[5] H. Poole, I. Saika-Voivod, and F. Sciortino, J. Phys.: Condens. Matter **17**, L431 (2005).
[6] M. Yamada, S. Mossa, H. Stanley, and F. Sciortino, Phys. Rev. Lett. **88**, 195701 (2002).
[7] L. Xu, P. Kumar, S. V. Buldyrev, S. Chen, P. H. Poole, F. Sciortino, and H. E. Stanley, Proc. Natl. Acad. Sci. U.S.A. **102**, 16558 (2005).
[8] Y. Liu, A. Z. Panagiotopoulos, and P. G. Debenedetti, J. Chem. Phys. **131**, 104508 (2009).
[9] D. Corradini, M. Rovere, and P. Gallo, J. Chem. Phys. **132**, 134508 (2010).
[10] J. L. F. Abascal and C. Vega, J. Chem. Phys. **133**, 234502 (2010).
[11] J. L. F. Abascal and C. Vega, J. Chem. Phys. **134**, 186101 (2011).
[12] D. T. Limmer and D. Chandler, J. Chem. Phys. **135**, 134503 (2011).
[13] F. Sciortino, I. Saika-Voivod, and P. Poole, Phys. Chem. Chem. Phys. **13**, 19759 (2011).
[14] P. H. Poole, S. R. Becker, F. Sciortino, and F. W. Starr, J. Phys. Chem. B **115**, 14176 (2011).
[15] T. A. Kesselring, G. Franzese, S. V. Buldyrev, H. J. Herrmann, and H. E. Stanley, Sci. Rep. **2**, 474 (2012).
[16] P. Gallo and F. Sciortino, "Ising universality class for the liquid-liquid critical point of one component fluid: A finite-size scaling test," Phys. Rev. Lett. (in press).
[17] V. Holten and M. Anisimov, e-print arXiv:1207.2101 [physics.chem-ph].
[18] O. Mishima, L. D. Calvert, and E. Whalley, Nature (Nature) **76**, 314 (1985).
[19] K. Winkel, M. Elsaesser, E. Mayer, and T. Loerting, J. Chem. Phys. **128**, 044510 (2008).
[20] C. U. Kim, B. Barstow, M. V. Tate, and S. M. Gruner, Proc. Natl. Acad. Sci. U.S.A. **106**, 4596 (2009).
[21] O. Mishima and H. E. Stanley, Nature (Nature) **392**, 164 (1998).
[22] O. Mishima and H. E. Stanley, Nature (Nature) **396**, 329 (1998).
[23] P. Gallo, F. Sciortino, P. Tartaglia, and S.-H. Chen, Phys. Rev. Lett. **76**, 2730 (1996).
[24] F. Sciortino, P. Gallo, P. Tartaglia, and S.-H. Chen, Phys. Rev. E **54**, 6331 (1996).
[25] W. Götze, *Complex Dynamics of Glass-Forming Liquids: A Mode-Coupling Theory* (Oxford University Press, Oxford, 2009).
[26] V. Krakoviack, Phys. Rev. Lett. **94**, 065703 (2005).
[27] S. Lang, R. Schilling, V. Krakoviack, and T. Franosch, Phys. Rev. E **86**, 021502 (2012).
[28] P. Gallo, M. Rovere, and E. Spohr, Phys. Rev. Lett. **85**, 4317 (2000).
[29] P. Gallo, M. Rovere, and E. Spohr, J. Chem. Phys. **113**, 11324 (2000).
[30] M. Ricci, F. Bruni, P. Gallo, M. Rovere, and A. Soper, J. Phys.: Condens. Matter **12**, A345 (2000).
[31] P. Gallo, M. Rovere, and S.-H. Chen, J. Phys. Chem. Lett. **1**, 729 (2010).
[32] P. Gallo, M. Rovere, and S.-H. Chen, J. Phys.: Condens. Matter **24**, 064109 (2012).
[33] A. Faraone, L. Liu, C.-Y. Mou, C.-W. Yen, and S.-H. Chen, J. Chem. Phys. **121**, 10843 (2004).
[34] L. Liu, S.-H. Chen, A. Faraone, C.-W. Yen, and C.-Y. Mou, Phys. Rev. Lett. **95**, 117802 (2005).
[35] A. Faraone, K.-H. Liu, C.-Y. Mou, Y. Zhang, and S.-H. Chen, J. Chem. Phys. **130**, 134512 (2009).
[36] C. A. Angell, Science **267**, 1924 (1995).
[37] D. Limmer and D. Chandler, J. chem. Phys. **137**, 044509 (2012).
[38] M. Nakanishi, P. Griffin, E. Mamontov, and A. P. Sokolov, J. Chem. Phys. **136**, 124512 (2012).
[39] F. Mallamace, M. Broccio, C. Corsaro, A. Faraone, U. Wanderlingh, L. Liu, C. Y. Mou, and S.-H. Chen, J. Chem. Phys. **124**, 161102 (2006).
[40] S.-H. Chen, F. Mallamace, C. Y. Mou, M. Broccio, C. Corsaro, A. Faraone, and L. Liu, Proc. Natl. Acad. Sci. U.S.A. **103**, 12974 (2006).
[41] F. Mallamace, C. Branca, C. C. N. Leone, J. Spooren, H. E. Stanley, and S.-H. Chen, J. Phys. Chem. B **114**, 1870 (2010).
[42] P. Gallo, M. Rovere, and S.-H. Chen, J. Phys.: Condens. Matter **22**, 284102 (2010).
[43] D. Corradini, P. Gallo, S. V. Buldyrev, and H. Stanley, Phys. Rev. E **85**, 051503 (2012).
[44] V. V. Brazhkin and V. N. Ryzhov, J. Chem. Phys. **135**, 084503 (2011).
[45] V. V. Brazhkin, Y. D. Fomin, A. G. Lyapin, V. N. Ryzhov, and E. N. Tsiok, J. Phys. Chem. B **115**, 14112 (2011).
[46] H. O. May and P. Mausbach, Phys. Rev. E **85**, 031201 (2012).
[47] L. Jorgensen, J. Chandrasekhar, J. D. Madura, R. W. Impey, and M. L. Klein, J. Chem. Phys. **79**, 926 (1983).
[48] D. Corradini, P. Gallo, and M. Rovere, J. Chem. Phys. **128**, 244508 (2008).
[49] D. Corradini, M. Rovere, and P. Gallo, J. Chem. Phys. **130**, 154511 (2009).
[50] D. Corradini, M. Rovere, and P. Gallo, J. Phys. Chem. B **115**, 1461 (2011).
[51] P. Gallo, D. Corradini, and M. Rovere, Mol. Phys. **109**, 2069 (2011).
[52] C. Vega, J. L. F. Abascal, M. M. Conde, and J. L. Aragones, Faraday Discuss. **141**, 251 (2009).
[53] A. K. Soper and K. Weckström, Biophys. Chem. **124**, 180 (2006).
[54] D. Corradini and P. Gallo, J. Phys. Chem. B **115**, 14161 (2011).
[55] S. W. Lovesey, *Theory of Neutron Scattering from Condensed Matter* (Clarendon, Oxford, 1984), Vol. 1.
[56] L. A. Baez and P. Clancy, J. Chem. Phys. **101**, 9837 (1994).
[57] P. Gallo, R. Pellarin, and M. Rovere, Europhys. Lett. **57**, 212 (2002).
[58] P. Gallo, A. Attili, and M. Rovere, Phys. Rev. E **80**, 061502 (2009).